# Photoelectric Detection of Coherent Light in Filtered Background Light

Carl W. Helstrom *

Department of Applied Physics and Information Science

University of California, San Diego

La Jolla, California 92037

## ABSTRACT

Calculated is the probability of detecting coherent light in the presence of background light that has passed through a narrowband filter of either rectangular or Lorentz frequency characteristic. Both signal and background fall on a photoelectric surface whose emitted electrons are counted and subjected to a randomized decision procedure that yields a pre-assigned false-alarm probability.

* This research was carried out under Research Grant NGL-05-009-079 from the National Aeronautics and Space Administration

A photoelectric counter is to detect the signal from an ideal laser in the presence of incoherent background light. The incident light passes through a filter whose passband, of width W, is centered at the frequency $\Omega$ of the signal, and through a polarizer that removes all background light polarized in a plane perpendicular to that of the signal, after which the light falls on a photoelectric surface. The signal, when present, has constant amplitude during the entire interval $(-1/2\ T, 1/2\ T)$ of observation.

When the passband of the filter is so broad that $WT \gg 1$, the distribution of the number n of photoelectrons is approximately Poisson, and this is the usual assumption in analyzing the performance of laser radar receivers.[1] If the passband could be made so narrow that $WT \ll 1$, the number n would have a Bose or a Laguerre distribution, depending on whether the signal is absent or present. Detection probabilities under this condition have been published.[2] So narrow a passband is difficult to attain in practice, especially when the frequency of the signal may be uncertain because of Doppler shift. The probability of detection should be worked out for intermediate values of WT in order to assess the accuracy of calculations based on the simplifying assumptions $WT \ll 1$ or $WT \gg 1$. Some results of such an analysis are presented here.

Let V(t) represent the complex envelope of the plane-polarized light field at the photoelectric surface. The probability P(n) that exactly n photoelectrons are emitted during the interval $(-1/2\ T, 1/2\ T)$ is given by a modified Poisson distribution,

$$P(n) = \langle x^n e^{-x}/n! \rangle,$$

$$x = \alpha \int_{-T/2}^{T/2} |V(t)|^2 \, dt, \tag{1}$$

where $\alpha$ is a constant proportional to the quantum efficiency of the surface and to its area.[3] The average indicated by $\langle\ \rangle$ is taken over the ensemble of circular-complex Gaussian processes $V(t)$.

When the signal is present (hypothesis $H_1$),

$$V(t) = S(t) + N(t); \tag{2}$$

when it is not (hypothesis $H_0$), $V(t) = N(t)$. Here $S(t) = A\, e^{i\psi}$ represents the laser field of constant amplitude A and random phase $\psi$; $N(t)$ is the complex envelope of the linearly polarized background field. The complex autocovariance, or temporal coherence function, of the background $R\ell\; N(t)\, e^{i\Omega t}$ is

$$1/2\; \underset{\sim}{E}[N(t_1)\; N^*(t_2)] = \varphi(t_1 - t_2); \tag{3}$$

the spectral density

$$\Phi(\omega) = \int_{-\infty}^{\infty} \varphi(\tau)\, e^{-i\omega\tau} \, d\tau$$

of the background is proportional to $|\gamma(\omega)|^2$, where $\gamma(\omega)$ is the transfer function of the filter, angular frequencies $\omega$ being referred to the signal frequency $\Omega$ as origin.

By expanding the field $V(t)$ in terms of the orthonormal eigenfunctions $f_j(t)$ of the integral equation

$$\mu_j\, f_j(t) = \int_{-T/2}^{T/2} \varphi(t - s)\, f_j(s)\, ds/\varphi(0)T \tag{4}$$

it can be shown that the number n of photoelectrons can be written as[4]

$$n = \sum_{j=1}^{\infty} n_j, \tag{5}$$

where the $n_j$'s are statistically independent, integral-valued random variables having under hypothesis $H_0$ Bose distributions $p_j^{(0)}(n_j)$ and under hypothesis $H_1$ Laguerre distributions $p_j^{(1)}(n_j)$. These distributions are

$$p_j^{(0)}(m) = (1 - v_j)\, v_j^{\,m}, \qquad (H_0) \tag{6}$$

$$p_j^{(1)}(m) = (1 - v_j) \exp[-(1 - v_j)\, S_j] \times v_j^{\,m}\, L_m[-(1 - v_j)^2\, S_j/v_j], \; (H_1) \tag{7}$$

where

$$v_j = N_j/(1 + N_j), \tag{8}$$

$$N_j = N\mu_j, \tag{9}$$

$$S_j = S\sigma_j,$$

$$\sigma_j = \left| \int_{-T/2}^{T/2} S(t)\, f_j(t)\, dt \right|^2 \Big/ \int_{-T/2}^{T/2} |S(t)|^2\, dt, \tag{10}$$

N is the total average number of electrons in (-1/2 T, 1/2 T) due to the background, S is the total average number that would be ejected by the signal S(t) alone, and $L_m(x)$ is the m-th Laguerre polynomial. Here

$$\sum_{j=1}^{\infty} \mu_j = 1, \quad \sum_{j=1}^{\infty} \sigma_j = 1. \tag{11}$$

The distributions $P_0(n)$ and $P_1(n)$ of the total number n of electrons are easily computed digitally by convolving the component distributions in (6) and (7) for which $\mu_j$ and $\sigma_j$ are significantly greater than zero.

The detection probabilities have been calculated for a randomized detector that chooses $H_1$ (signal present) whenever the number $n$ of electrons exceeds a certain integral decision level $\theta$. When $n < \theta$, the detector chooses $H_0$ (signal absent). When $n = \theta$, hypothesis $H_1$ is chosen with probability $f$, $0 \le f < 1$. The values of $\theta$ and $f$ are selected so that the false-alarm probability

$$Q_0 = f\,P_0(\theta) + \sum_{k=\theta+1}^{\infty} P_0(k) \tag{12}$$

takes on a pre-assigned value. To find $f$ and $\theta$, $P_0(k)$ is summed from $k=0$ until the sum $\Sigma$ exceeds $1 - Q_0$. The value of $k$ at which this first happens is $\theta$, and

$$f = (\Sigma - 1 + Q_0)/P_0(\theta).$$

The probability $Q_d$ of detection is then given by

$$Q_d = f\,P_1(\theta) + \sum_{k=\theta+1}^{\infty} P_1(k). \tag{13}$$

(a) Rectangular Spectrum

When the filter has a rectangular frequency characteristic, the complex autocovariance of the background light striking the photosensitive surface is

$$\varphi(\tau) = \varphi(0) \sin(\pi W\tau)/(\pi W\tau), \tag{14}$$

and the integral equation (4) is the one treated by Slepian and Pollak.[5] The eigenfunctions are the angular prolate spheroidal wave functions

$$f_n(t) = u_n^{-1}(2/T)^{1/2} S_{0n}(c, 2t/T) \tag{15}$$

with $c = \pi WT/2$ and $u_n$ the normalization factor given by

$$u_n^2 = \int_{-1}^{1} |S_{0n}(c, x)|^2 \, dx. \tag{16}$$

In the notation of Stratton *et al.*,[6]

$$S_{0n}(c, x) = \sum_{k=0}^{\infty} d_k(c|0n) \, P_n(x) \tag{17}$$

in terms of the Legendre polynomials $P_n(x)$, and by their orthogonality over (-1, 1),

$$u_n^2 = 2 \sum_{k=0}^{\infty} (2k + 1)^{-1} \, [d_k(c|0n)]^2. \tag{18}$$

The eigenvalues of (4) are, in the notation of Slepian and Pollak,[5]

$$\mu_k = \lambda_k(c)/WT. \tag{19}$$

The quantities $\sigma_k$ in (10) are

$$\sigma_k = 2\mu_k u_k^{-2} |S_{0k}(c, 0)|^2, \tag{20}$$

for with S(t) constant over (-1/2 T, 1/2 T), we need only to evaluate the Fourier transform[7]

$$\int_{-T/2}^{T/2} f_n(t) e^{i\omega t} dt = u_n^{-1}[2\lambda_n(c)/W]^{1/2} S_{0n}(c, \omega/\pi W) \tag{21}$$

at $\omega = 0$. Here $\sigma_k = 0$ for k odd.

By using these formulas we calculated the distributions in (6) and (7), convolved them to determine the distributions $P_0(k)$ and $P_1(k)$, and used (12) and (13) to work out the probabilities of detection, which are plotted in Figs. 1 - 3 for various values of false-alarm probability $Q_0$, mean number N of background photoelectrons, and time-bandwidth product $c = \pi WT/2$. For a fixed background illuminance, the number N increases, and the probability $Q_d$ of detection decreases, as the bandwidth W of the filter increases. For our present purposes it seemed more instructive to avoid this trivial effect and keep the total average number N of electrons fixed. The detection probability then increases as the filter passband widens and the distributions become more nearly Poisson.

(b) Lorentz Spectrum

When the filter has the pass characteristic of a simply resonant linear system, the spectral density of the background light falling on the photosurface has the Lorentz form

$$\Phi(\omega) = 2W\, \varphi(0)\, (\omega^2 + W^2)^{-1}, \tag{22}$$

and its temporal coherence function is

$$\varphi(\tau) = \varphi(0)\, e^{-W|\tau|}. \tag{23}$$

The integral equation (4) is then easily solved; the eigenfunctions are sinusoidal.[8]

The eigenvalues $\mu_k$ do not drop off with increasing k rapidly enough to make it feasible to calculate the distribution $P_0(k)$ by convolution. Instead we determined it by an ingenious recurrent equation due to G. Bédard.[9] The generating function of the distribution $\{P_1(k)\}$ has the form[4]

$$g_1(s) = \sum_{k=0}^{\infty} P_1(k)\, z^k =$$

$$g_0(s) \prod_{j=1}^{\infty} \exp\{-(1 - s)\, S_j/[1 + N_j(1 - s)]\}, \tag{24}$$

where $g_0(s)$ is the generating function of $\{P_0(k)\}$. We can determine $\{P_1(k)\}$, therefore, by convolving the sequence $\{P_0(k)\}$, k = 0, 1, 2,..., with the quasi-distributions $\{q_j(k)\}$ whose generating functions are the exponential factors in (24). These quasi-distributions are given by

$$q_j(k) = v_j^k \exp[-(1 - v_j)\, S_j] \quad L_k^{(-1)}[-(1 - v_j)^2\, S_j/v_j], \tag{25}$$

where $L_k^{(-1)}(x)$ is a generalized Laguerre polynomial.[10] It can easily be computed from its recurrent equation,

$$(k + 1)\ L_{k+1}^{(-1)}(x) = (2k - x)\ L_k^{(-1)}(x) - (k - 1)\ L_{k-1}^{(-1)}(x),$$

$$L_0^{(-1)}(x) = 1, \qquad L_1^{(-1)}(x) = -x. \tag{26}$$

In this calculation only the even eigenfunctions $f_k(t)$ need to be included,

$$f_k(t) = u_k^{-1} \cos w_k t; \tag{27}$$

the odd ones yield $\sigma_j = 0$ in (10). The eigenvalues $\mu_k$ are now[8]

$$\mu_k = m(m^2 + \theta_k^2)^{-1}, \qquad m = WT/2, \tag{28}$$

where $\theta_k$ is the k-th root of the transcendental equation

$$\theta_k \tan \theta_k = m, \qquad \theta_k = w_k T/2, \tag{29}$$

which is easily solved by Newton's method. The normalization constant $u_k$ is given by

$$u_k^2 = \theta_k(1 + \mu_k)/w_n, \tag{30}$$

and

$$\sigma_k = 2m\ \mu_k\ \theta_k^{-2}\ (1 + \mu_k)^{-1}. \tag{31}$$

The detection probabilities for various values of WT are plotted in Figs. 4-6. The curves have the same general behavior as those for the rectangular spectrum.

References

1. J. W. Goodman, "Comparative Performance of Optical-Radar Detection Techniques", Trans. IEEE, vol. AES-2, pp. 526-535; Sept. 1966.

2. C. W. Helstrom, "Performance of an Ideal Quantum Receiver of a Coherent Signal of Random Phase", Trans. IEEE, vol. AES-5, pp. 562-564; May, 1969.

3. L. Mandel, "Fluctuations of Photon Beams and their Correlations", Proc. Phys. Soc. (London), vol. 72, pp. 1037-1048; December, 1958.

4. S. Karp, J. R. Clark, "Photon Counting: A Problem in Classical Noise Theory", Trans. IEEE, vol. IT-16, pp. ; November, 1970.

5. D. Slepian, H. O. Pollak, "Prolate Spheroidal Wave Functions, Fourier Analysis and Uncertainty, I", Bell System Tech. J., vol. 40, pp. 43-63; January, 1961.

6. J. A. Stratton, P. M. Morse, L. J. Chu, J. D. C. Little, F. J. Corbató, Spheroidal Wave Functions; M.I.T. Press, 1956.

7. Reference 5, Eq. (25), p. 57.

8. C. W. Helstrom, Statistical Theory of Signal Detection, 2nd. ed.; Pergamon Press, London, 1968. See Ch. IV, Sec. 5, pp. 138-141.

9. G. Bédard, "Photon Counting Statistics of Gaussian Light", Phys. Rev., vol. 151, pp. 1038-1039; Nov. 25, 1966.

10. A. Erdélyi *et al.*, Higher Transcendental Functions; McGraw-Hill Book Co., New York, 1953. See vol. 2, Sec. 10.12, pp. 188-192.

## Figure Captions

Fig. 1. Probability of detection vs. average number S of signal counts for rectangular background spectrum; $Q_0 = 10^{-2}$, N = 0.5. The curves are indexed with the value of $c = \pi WT/2$.

Fig. 2. Probability of detection vs. average number S of signal counts for rectangular background spectrum; $Q_0 = 10^{-2}$, N = 2.0. The curves are indexed with the value of $c = \pi WT/2$.

Fig. 3. Probability of detection vs. average number S of signal counts for rectangular background spectrum; $Q_0 = 10^{-4}$, N = 0.5. The curves are indexed with the value of $c = \pi WT/2$.

Fig. 4. Probability of detection vs. average number S of signal counts for Lorentz background spectrum; $Q_0 = 10^{-2}$, N = 0.5. The curves are indexed with the value of WT.

Fig. 5. Probability of detection vs. average number S of signal counts for Lorentz background spectrum; $Q_0 = 10^{-2}$, N = 2.0. The curves are indexed with the value of WT.

Fig. 6. Probability of detection vs. average number S of signal counts for Lorentz background spectrum; $Q_0 = 10^{-4}$, N = 0.5. The curves are indexed with the value of WT.

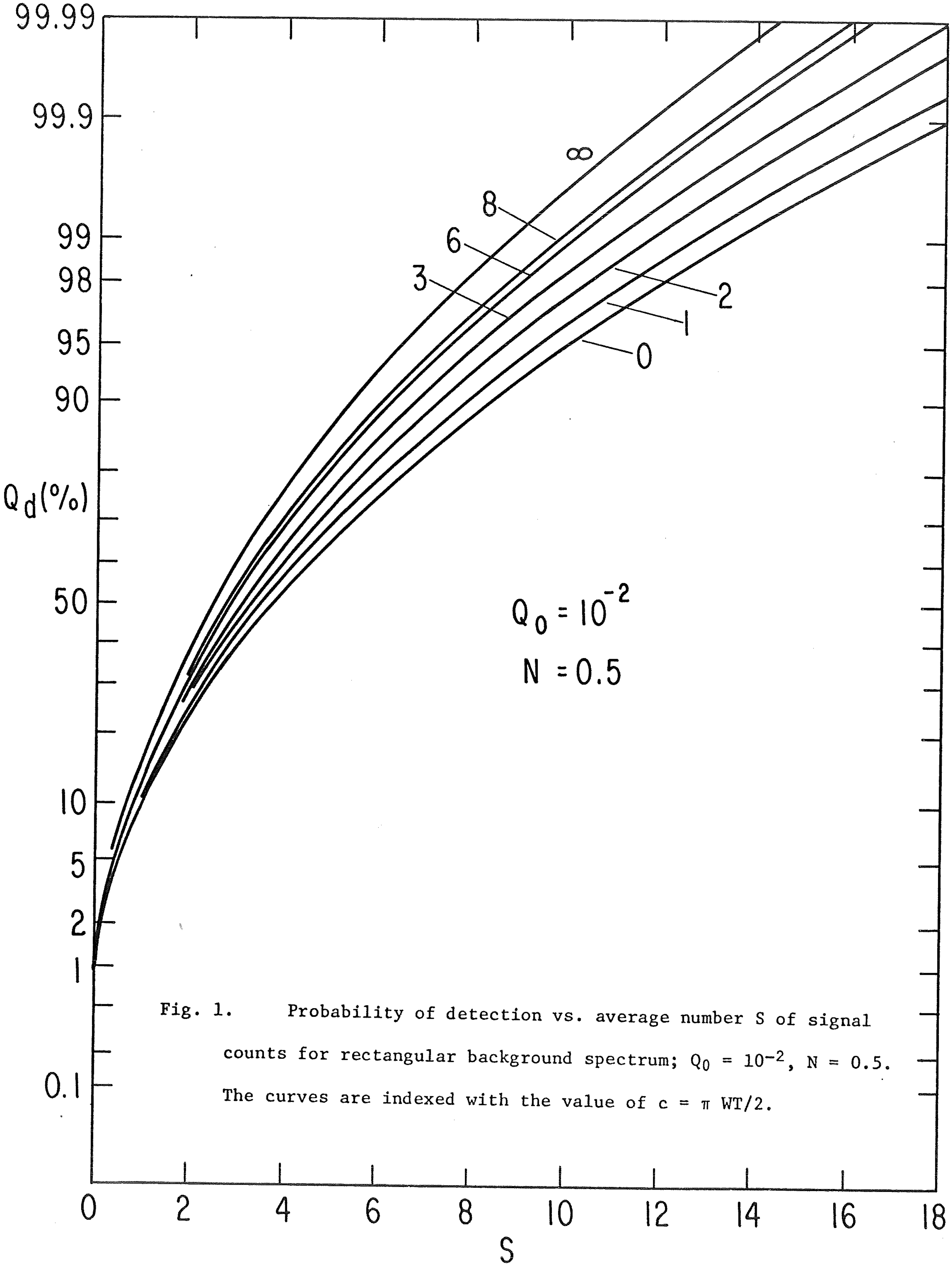


Fig. 1. Probability of detection vs. average number S of signal counts for rectangular background spectrum; $Q_0 = 10^{-2}$, N = 0.5. The curves are indexed with the value of $c = \pi WT/2$.

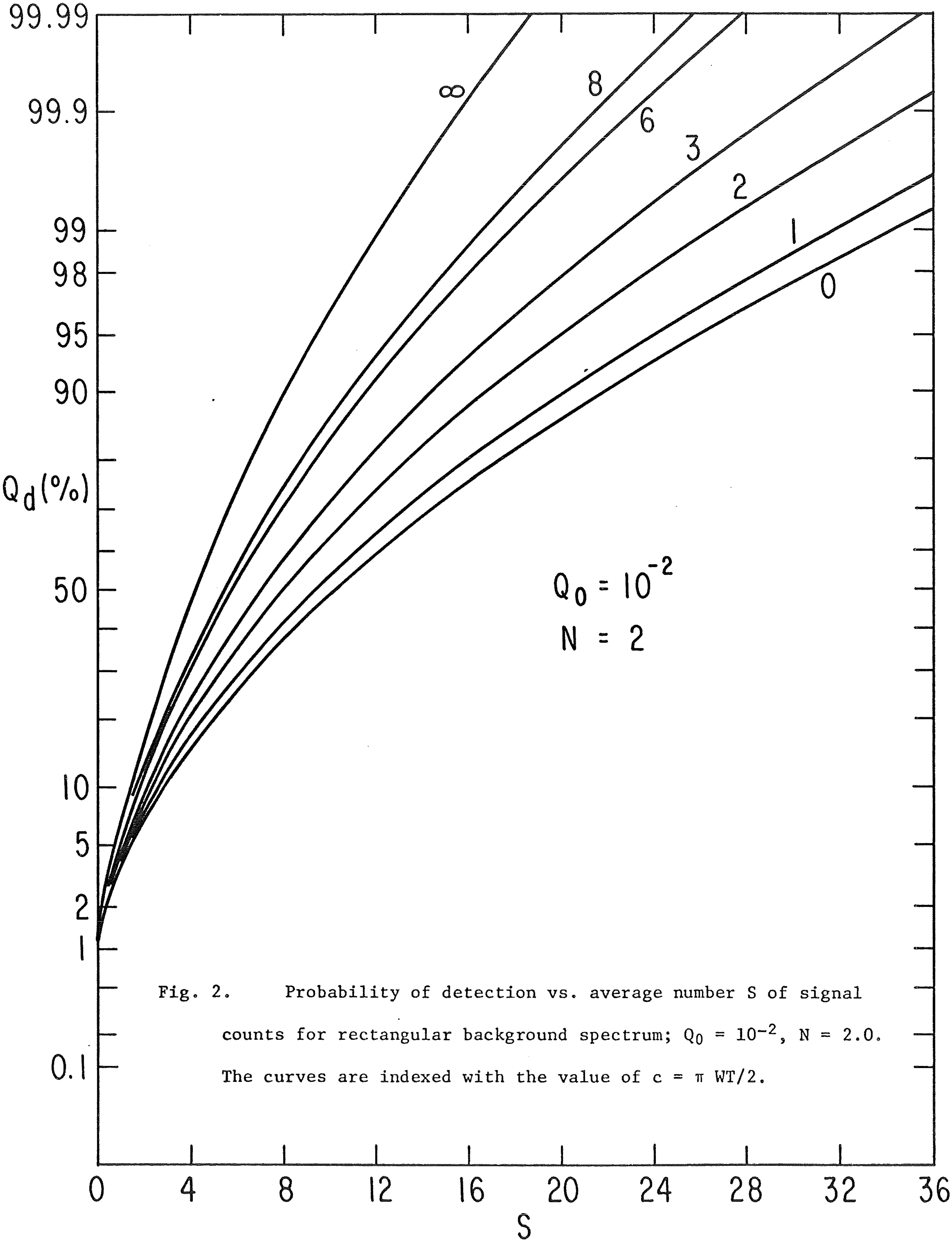


Fig. 2. Probability of detection vs. average number S of signal counts for rectangular background spectrum; $Q_0 = 10^{-2}$, N = 2.0. The curves are indexed with the value of $c = \pi WT/2$.

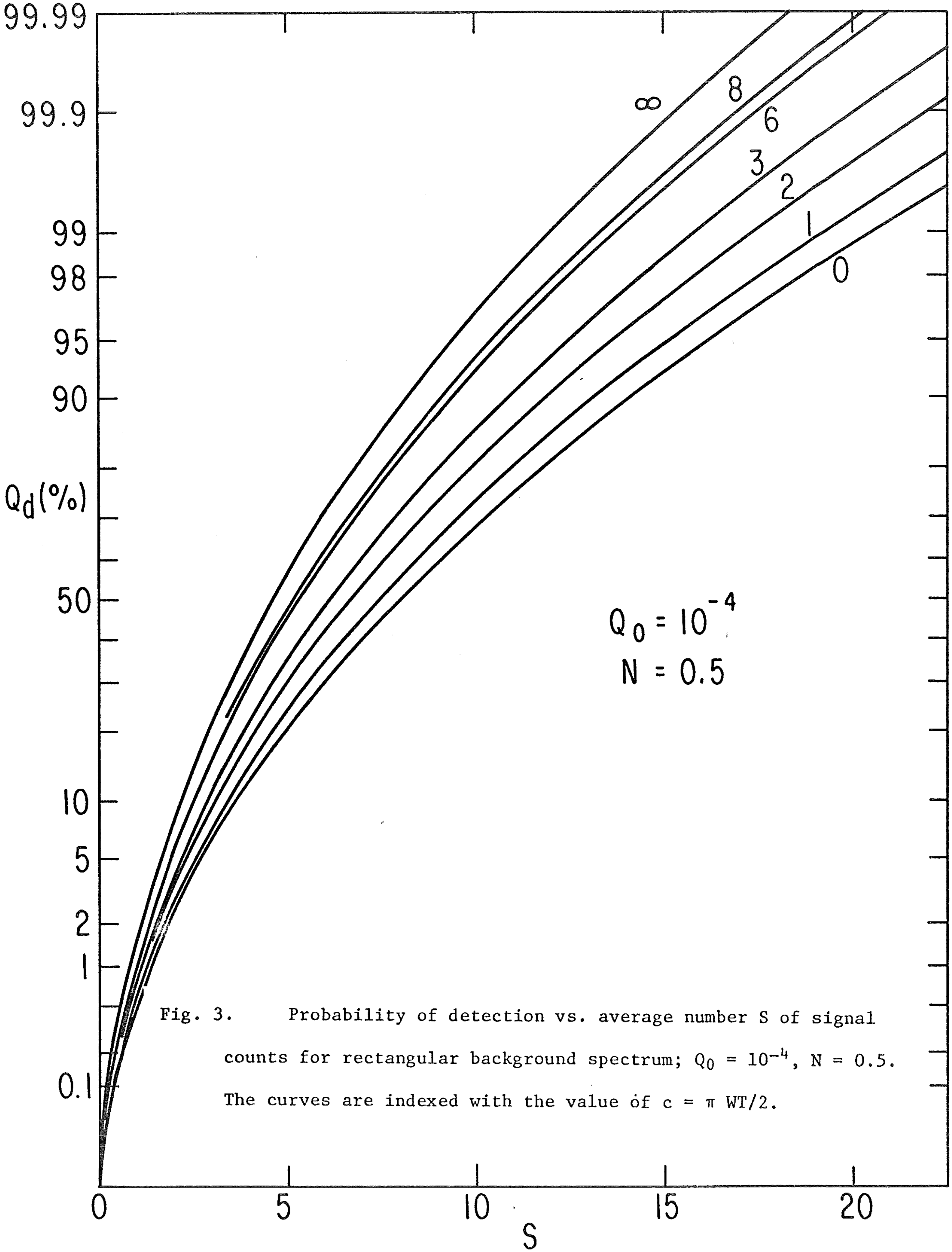


Fig. 3. Probability of detection vs. average number S of signal counts for rectangular background spectrum; $Q_0 = 10^{-4}$, N = 0.5. The curves are indexed with the value of $c = \pi WT/2$.

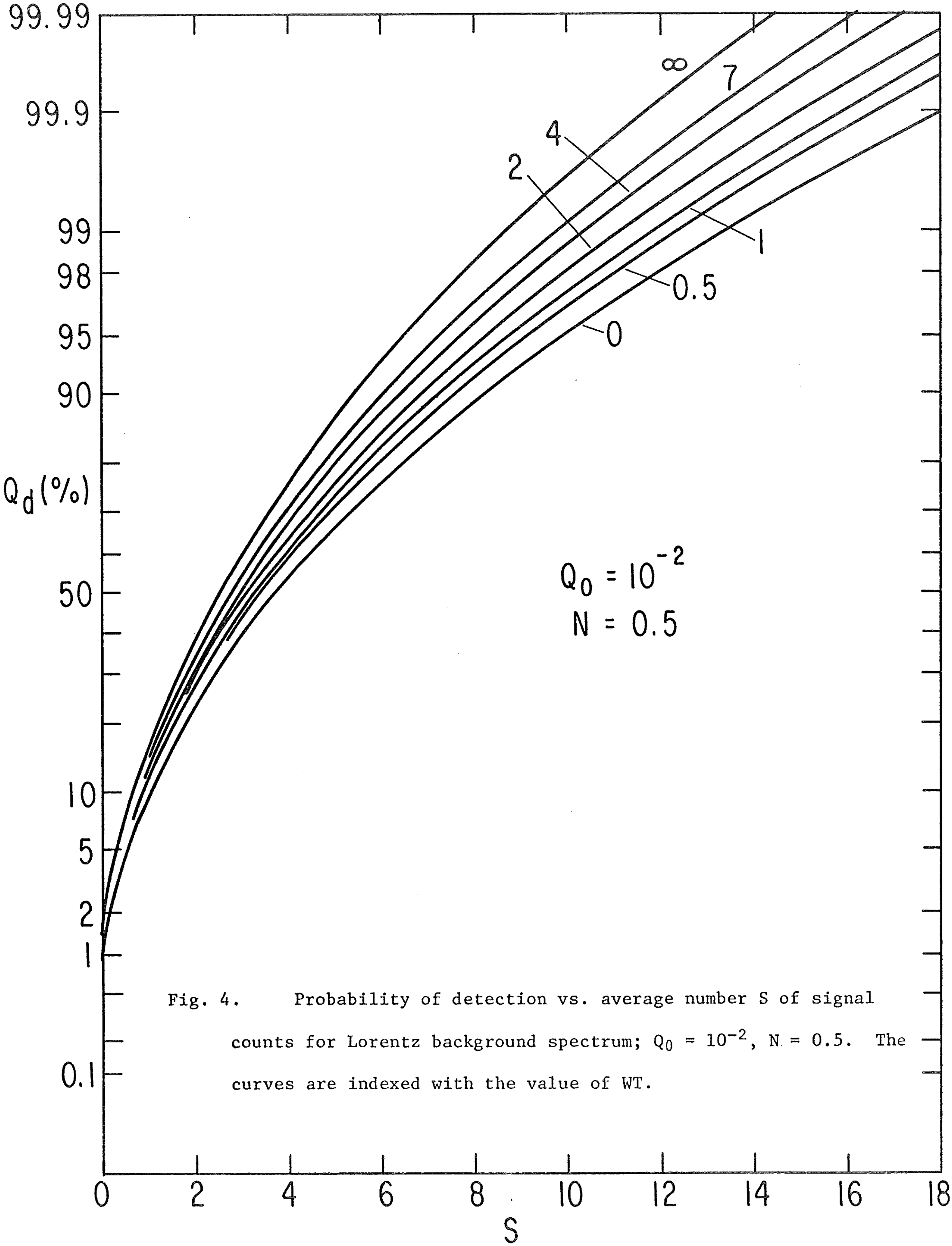


Fig. 4. Probability of detection vs. average number S of signal counts for Lorentz background spectrum; $Q_0 = 10^{-2}$, N = 0.5. The curves are indexed with the value of WT.

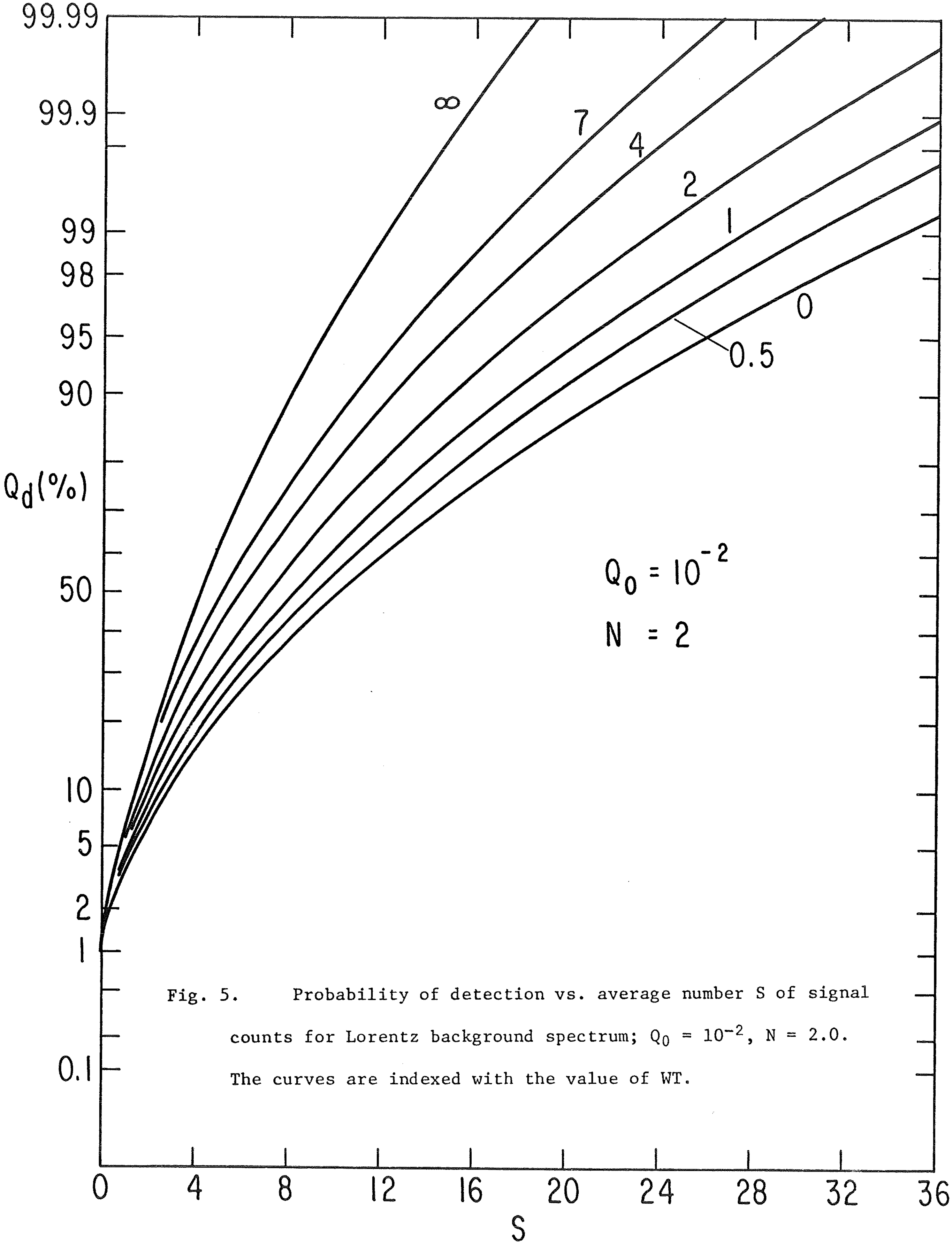


Fig. 5. Probability of detection vs. average number S of signal counts for Lorentz background spectrum; $Q_0 = 10^{-2}$, N = 2.0. The curves are indexed with the value of WT.

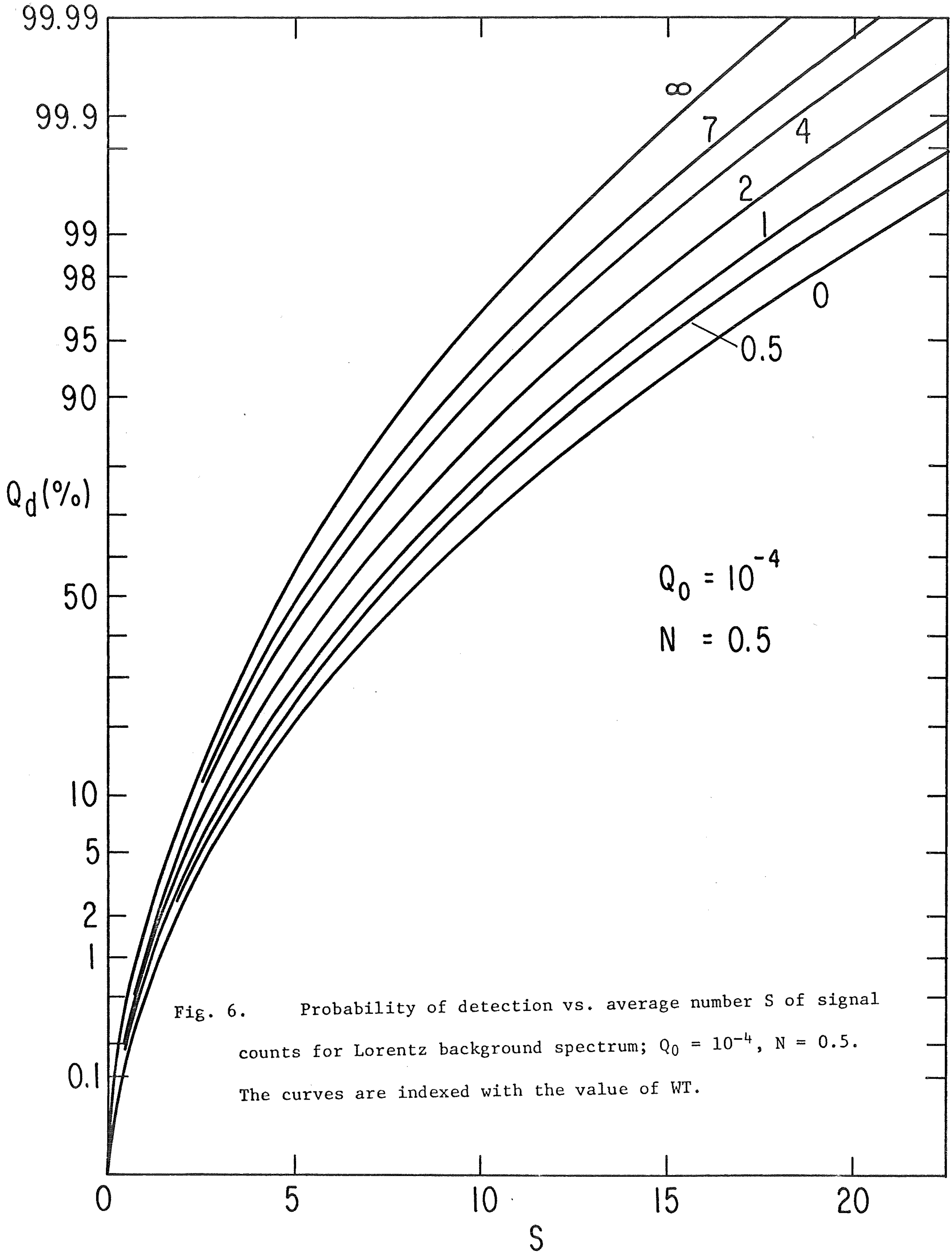


Fig. 6. Probability of detection vs. average number S of signal counts for Lorentz background spectrum; $Q_0 = 10^{-4}$, N = 0.5. The curves are indexed with the value of WT.